Principal Component Analysis Accelerated the Iterative Convergence of the Characteristic Mode Basis Function Method for Analyzing Electromagnetic Scattering Problems

Zhonggen Wang[1], Fei Guo[1, *], Wenyan Nie[2], Yufa Sun[3], and Pan Wang[1]

Abstract—According to the characteristic mode basis function method (CMBFM) in analyzing electrically large problems, blocking and extending lead to the problem of slow convergence in the iterative solution of a reduced matrix equation, and the characteristic mode basis function method combined with principal component analysis (CMBFM-PCA) is proposed in this study. The characteristic modes (CMs), calculated from each extended block, are subjected to PCA to enhance the orthogonality between them and improve the reduced matrix's condition number to facilitate its quick convergence through an iterative solution. The corresponding numerical calculations demonstrate that significant efficiency and accuracy are achieved by the proposed method.

1. INTRODUCTION

As a rigorous numerical calculation method, the method of moments (MoM) [1] is widely used in the numerical calculation of electromagnetic fields and is regarded as an evaluation standard. However, the MoM is limited in solving and storing the full rank matrix when the size of the object increases. To decrease the computational effort and accelerate the solution of the equations, various efficient and fast algorithms have been proposed, such as the adaptive integration method (AIM) [2], adaptive cross approximation (ACA) [3], multi-level adaptive cross approximation (MLACA) [4], and multi-level fast multipole method (MLFMM) [5]. Despite that these methods could accelerate the vector product of the matrix, problems still resided in reducing the computational complexity of the algorithms to effectively deal with electrically large objects. For the latter, the macro basis function was introduced to reduce the matrix dimension; more precisely, one of the representative algorithms was the characteristic basis function method (CBFM) [6]. Therefore, based on the principle of domain decomposition, CBFM divides the object into multiple blocks. By constructing the characteristic basis functions (CBFs) and considering the coupling between blocks, the matrix equation is transformed into a reduced matrix equation with low dimensionality. However, the generation of CBFs requires a lot of incident excitations, and the construction of CBFs consumes a huge time.

Therefore, characteristic mode (CM) is an intrinsic mode, adapted to an arbitrary electromagnetic structure, independent of the applied excitation and related solely to the shape and material of the structure [7]. According to the CM theory, the surface current or the radiation pattern of any object can be decomposed into a superposition of a series of characteristic currents or characteristic far fields associated with the CMs. Thus, the CM theory is widely used to find or construct one or multiple modes whose resonant frequency, current distribution, radiation pattern, and gain can satisfy the performance

[1] School of Electrical and Information Engineering, Anhui University of Science and Technology, Huainan 232001, China. [2] School of Mechanical and Electrical Engineering, Huainan Normal University, Huainan 232001, China. [3] School of Electronics and Information Engineering, Anhui University, Hefei 230039, China.

requirements of the antenna [8–10], while it is rarely applied to the analysis of electromagnetic scattering problems.

As for the existent tools and algorithms, the traditional characteristic mode method (CMM) [11] has low efficiency in analyzing electrically large scattering problems due to its high complexity in solving the CMs. To improve the analysis efficiency of electromagnetic scattering problems, Ref. [12] proposed the characteristic mode basis function method (CMBFM), which calculated the CMs of each extended block separately by blocking objects and improved the overall efficiency of constructing CMs along with the reduction of the matrix dimension. However, it was difficult to apply this method to electrically large problems due to the poor condition number of the reduced matrix. Consequently, based on blocking, Ref. [13] introduced a matrix preconditioning technique to accelerate the iterative solution of the reduced matrix equation; however, the number of generated basis functions and the matrix dimension were large and yielded a complex calculation. In addition, Ref. [14] introduced the MLFMM algorithm while using a message-passing interface parallel strategy to save computational time. Regrettably, the issues of large matrix dimension and the deteriorated condition number of the reduced matrix remained unresolved. Similarly, Ref. [15] extracted CMs from the impedance matrix, generated by the augmented electric field integral equation, and achieved the unitization of CMs by blocking to decrease unknowns, while using MLFMM to accelerate the filling of the matrix. Nevertheless, the dimension of the reduced matrix has not been effectively diminished. More particularly, the CM theory was combined with compressive sensing, and it was used to analyze the bistatic scattering of three-dimensional objects as proposed by [16]; however, the number of basis functions and the dimensionality of the measurement matrix were large.

In this paper, a novel algorithm, based on characteristic mode basis function method combined with the principal component analysis (CMBFM-PCA), is proposed for analyzing the electromagnetic scattering problems of electrically large objects. Based on retaining the block and extension operations of the CMBFM, which assures the efficiency of solving the CMs, a combining with PCA [17] alleviates the problem of the orthogonality deterioration between these CMs. Moreover, by applying PCA to the CMs, the condition number of the constructed reduced matrix is optimized, thereby improving the efficiency of solving the reduced matrix equation. The effectiveness of the proposed method is verified by comprehensive numerical simulations.

2. FORMULATION

2.1. Characteristic Mode Basis Function Method

MoM was widely used for solving electromagnetic scattering problems owing to its high solution accuracy and unnecessity of setting absorption boundary conditions. Moreover, it was expressed as follows:

$$\mathbf{Z}\mathbf{J} = \mathbf{V} \tag{1}$$

where $\mathbf{Z}$ represents the impedance matrix, and $\mathbf{J}$ and $\mathbf{V}$ are the current coefficient vector and excitation vector, respectively.

Based on the CM theory developed for perfect electric conductors (PEC), the CMs were determined by solving the generalized eigenvalue equation. However, the equation requires a high solution complexity, leading to decreasing the efficiency of solving the CMs. To alleviate this problem, the CMBFM initially divided the object into M blocks to achieve the blocking of the impedance matrix and the discretization of the unknowns. Hence, the efficiency of solving CMs was improved by decreasing the matrix dimension. Unfortunately, although blocking could improve the efficiency of solving CMs, it also yielded in changing the shape of the object; therefore, the CMs of each block would change accordingly, especially for those near the virtual boundary. For this reason, each block was extended to ensure the continuity and smoothness of the characteristic currents near the virtual boundary. As a result, Eq. (1) can be rewritten as follows:

$$\begin{bmatrix} \mathbf{Z}_{11} & \mathbf{Z}_{12} & \cdots & \mathbf{Z}_{1M} \\ \mathbf{Z}_{21} & \mathbf{Z}_{22} & \cdots & \mathbf{Z}_{2M} \\ \vdots & \vdots & \ddots & \vdots \\ \mathbf{Z}_{M1} & \mathbf{Z}_{M2} & \cdots & \mathbf{Z}_{MM} \end{bmatrix} \begin{bmatrix} \mathbf{J}_1 \\ \mathbf{J}_2 \\ \vdots \\ \mathbf{J}_M \end{bmatrix} = \begin{bmatrix} \mathbf{V}_1 \\ \mathbf{V}_2 \\ \vdots \\ \mathbf{V}_M \end{bmatrix} \tag{2}$$

where $\mathbf{Z}_{ii}$ and $\mathbf{Z}_{ij}$ represent the self-impedance matrix and mutual impedance matrix with the dimension of $N_i^e \times N_i^e$ and $N_i^e \times N_j^e$, respectively. In addition, N_i^e and N_j^e indicate the unknowns in blocks i and j, respectively, where superscript e denotes the extension symbol. Besides, $\mathbf{J}_i$ and $\mathbf{V}_i$ represent the current and excitation on block i, respectively. Therefore, for the extended block i, its CMs were obtained by calculating the extended self-impedance matrix $\mathbf{Z}_{ii}^e$ that is expressed as follows:

$$\mathbf{Z}_{ii}^e = \mathbf{R}_{ii}^e + j\mathbf{X}_{ii}^e \tag{3}$$

$$\mathbf{X}_{ii}\mathbf{J}_i^e = \lambda_i \mathbf{R}_{ii}\mathbf{J}_i^e \tag{4}$$

where $\mathbf{R}_{ii}^e$ and $\mathbf{X}_{ii}^e$ are the real and imaginary parts of $\mathbf{Z}_{ii}^e$, respectively, and $\mathbf{J}_i^e$ is the eigenvector associated with the eigenvalue λ_i, also known as the CM.

It is worth noting that the linear superposition of a few low-order CMs is sufficient to approximate the surface current of the object due to its properties. In this sense, these low-order mode currents were selected as the characteristic mode basis functions (CMBFs). Thus, the selection strategy of CMs was determined by the mode significance (MS), defined as follows:

$$\mathrm{MS} = \left| \frac{1}{1 + j\lambda_i} \right| \tag{5}$$

Moreover, a threshold τ_{cm} was determined with respect to the MS value. Therefore, a group of significant eigenvalues λ_i was obtained when $\mathrm{MS} > \tau_{cm}$, and the corresponding significant CMs were used as CMBFs of block i. Finally, it is assumed that the number of CMBFs on the block i is K_i; thus the current of the block i is expressed as follows:

$$\mathbf{J}_i = \sum_k^{K_i} a_i^k \mathbf{J}_i^{CM_k} \tag{6}$$

where a_i^k represents the coefficient matrix to be solved, and $\mathbf{J}_i^{CM_k}$ is the kth CMBFs of block i. Afterwards, a reduced matrix is built to compute a_i^k by using the Galerkin method defined as follows:

$$\mathbf{Z}^R = \left(\mathbf{J}^{CM}\right)^T \mathbf{Z}\mathbf{J}^{CM} \tag{7}$$

$$\mathbf{Z}^R a = \mathbf{V}^R \tag{8}$$

where $\mathbf{J}^{CM}$ is a matrix that contains all CMBFs, $\mathbf{Z}^R$ a reduced matrix with the dimension of $\sum_{i=1}^{M} K_i \times \sum_{i=1}^{M} K_i$, and $\mathbf{V}^R$ an excitation vector. Furthermore, a is the matrix of extension coefficients obtained by solving Eq. (8).

However, with the increasing number of unknowns, the reduced matrix equation needs to be solved by the iterative method. Unfortunately, the CMBFM ensures the efficiency and accuracy of computation by blocking and extending while weakening the orthogonality among CMBFs. As a result, the condition number of the reduced matrix becomes worse, and the iterative solution slowly converges.

2.2. Characteristic Mode Basis Function Method Combined with Principal Component Analysis

PCA is a multivariate statistical analysis method [18, 19], which transforms a group of potentially correlated variables into a group of linearly uncorrelated ones using the orthogonal transformation. The purpose of this method is to enhance the orthogonality between vectors and reduce the dimension of the matrix. PCA identifies the main directions of variance in the data by orthogonal transformation and projects the original data onto these directions. By setting an appropriate threshold, it is possible to retain as much information as possible from the principal components in the main directions. The data are projected onto these principal components to achieve dimensionality reduction while enhancing the orthogonality between the data. This interpretation is particularly important for data analysis. In addition, the principal component extracted by PCA represents the direction of maximum variance in the data, thereby capturing the underlying trend and features of the data to a significant extent. Therefore, to improve the condition number of the reduced matrix and boost the convergence rate of the iterative solution, PCA was used to process the effective CMs selected by MS.

Moreover, to alleviate the time-consuming PCA process caused by the excessive number of CMs and the large matrix dimension, PCA was performed on each block separately after removing the extension. As a result, it was assumed that the matrix, consisting of CMs on a block i, arranged by rows, was represented by a matrix $\mathbf{R}_i$ of dimension $n \times p$, where n and p denote the number of CMs and unexpended unknowns on the block i, respectively. After normalization, the covariance of $\mathbf{R}_i$ was calculated, and the matrix was constructed as follows (the superscript T indicates transposition):

$$\mathbf{C}_i = \frac{1}{n-1}\mathbf{R}_i\mathbf{R}_i^T \tag{9}$$

where $\mathbf{C}_i$ is the covariance matrix having a dimension of $n \times n$. Afterwards, the singular value decomposition (SVD) of $\mathbf{C}_i$ is performed to obtain the eigenvalues and eigenvectors, and these eigenvectors are the principal components. The process of SVD is defined as follows:

$$\mathbf{C}_i = \mathbf{U}\mathbf{D}\mathbf{V}^T \tag{10}$$

where $\mathbf{U}$ and $\mathbf{V}^T$ are both orthogonal matrixes, and $\mathbf{D}$ is a diagonal matrix whose elements are arranged from the largest to the smallest with a rapid decay trend, all of which are singular values of $\mathbf{C}_i$. By specifying a suitable threshold value σ for $\mathbf{U}$ and choosing the left singular vectors that exceed the threshold, the linear combination of these selected vectors is represented by the matrix $\mathbf{W}_i$. Therefore, $\mathbf{R}_i$ is handled by PCA to generate the reduced dimensional $\mathbf{R}_i^*$ denoted as follows:

$$\mathbf{R}_i^* = \mathbf{W}_i^T\mathbf{R}_i \tag{11}$$

Moreover, $\mathbf{R}_i^*$ is transposed to obtain $\mathbf{J}_i^N$. The column vector in $\mathbf{J}_i^N$ represents the new characteristic mode basis functions (NCMBFs). Considering that the number of NCMBFs, retained by the CMs over the block i after applying PCA handling is Q_i, the current on the present block can be expressed as follows:

$$\mathbf{J}_i = \sum_{q=1}^{Q_i} a_i^q \mathbf{J}_i^{NCM_q} = \mathbf{J}_i^{NCM} a_i \tag{12}$$

where a_i^q is the coefficient matrix to be solved, and $\mathbf{J}_i^{NCM_q}$ is the qth NCMBFs of the block i. Based on this, the original current of the object is expressed as follows:

$$\mathbf{J} = \begin{bmatrix} \mathbf{J}_1^{NCM} & 0 & \cdots & 0 \\ 0 & \mathbf{J}_2^{NCM} & \cdots & 0 \\ \vdots & \vdots & \ddots & \vdots \\ 0 & 0 & \cdots & \mathbf{J}_M^{NCM} \end{bmatrix} \begin{bmatrix} a_1 \\ a_2 \\ \vdots \\ a_M \end{bmatrix} = \mathbf{J}^{NCM} a \tag{13}$$

where a is obtained by solving the reduced matrix with the size of $\sum_{i=1}^{M} Q_i \times \sum_{i=1}^{M} Q_i$.

Compared to the CMBFM, the PCA enhances the orthogonality among NCMBFs by applying the orthogonal transformation in CMBFM-PCA; moreover, the condition number of the reduced matrix constructed by NCMBFs is significantly improved. Meanwhile, the complexity of iteratively solving the reduced matrix equation is $O\left(N_{iter}N_r^2\right)$, where N_r represents the dimensionality of the reduced matrix, and N_{iter} represents the number of iterations needed to finalize the simulation. Concerning CMBFM-PCA, the condition number of the reduced matrix is better, and N_r and the required N_{iter} are smaller, so the complexity is lower. For this reason, CMBFM-PCA can achieve faster convergence and decrease the computational cost in terms of analysis of electrically large problems.

3. NUMERICAL RESULTS

To test the performance of CMBFM-PCA, numerical simulations are performed at two different levels by using CMBFM and CMBFM-PCA. In addition, the generalized minimum residual (GMRES) method is considered as the iterative algorithm, and the incomplete LU (iLU) decomposition is used for preconditioning. The tolerances of GMRES and iLU decomposition are empirically set to 1E-5 and 0.001,

respectively. In this paper, the relative error is deployed to evaluate the accuracy of the results calculated by two methods, and it is defined as follows:

$$\text{Err} = \frac{\|\sigma_{\text{cal}} - \sigma_{\text{MoM}}\|_2}{\|\sigma_{\text{MoM}}\|_2} \times 100\% \tag{14}$$

where σ_{cal} and σ_{MoM} represent the radar cross section (RCS), calculated via the used method and MoM, respectively.

3.1. PEC Cylinder

Initially, the bistatic RCS is calculated for a cylinder with a radius of 0.2 m and a height of 1 m at a frequency of 1.8 GHz. The surface of the cylinder is discretized by the Rao-Wilton-Glisson (RWG) functions to produce 18478 triangles and 27711 unknowns. By dividing the target into 16 blocks where each block is extended by 0.15λ, the unknowns after the extension are 65457.

To evaluate the effects of the different extension sizes on the response accuracy, the root-mean-square error (RMSE) of CMBFM-PCA varies as shown in Fig. 1. On the other hand, the variation of the number of NCMBFs with τ_{cm} under different extension sizes is shown in Fig. 2. It is noticed that as the extension size increases, the number of basis functions grows, and the accuracy subsequently improves. Moreover, the larger the size of the extension is, the longer the time required will be. As a result, to balance the time and accuracy, the extended size is set to 0.15λ, and τ_{cm} is set to 0.001, respectively. Subsequently, the condition numbers of the reduced matrix for CMBFM and CMBFM-PCA are calculated separately using the same threshold but different extension sizes, as shown in Table 1. Referring to this table, it can be observed that as the extension size gradually increases, the condition number of the reduced matrix deteriorates, ultimately resulting in an ill-conditioned matrix. By setting different thresholds for PCA, the variations in the number of basis functions and error under different thresholds are observed as shown in Fig. 3. It can be found that as the threshold increases, the trend of the computation error decreases gradually. However, the number of retained basis functions gradually increases, which consumes computational time. Setting the threshold σ to 0.968 can not only ensure the accuracy of the algorithm, but also reduce the number of basis functions and provide strong stability. Therefore, in CMBFM-PCA, the CMBFs act as NCMBFs after performing the PCA with the threshold σ set to 0.968, and the orthogonality among NCMBFs is enhanced. As a result, the condition number of the reduced matrix, constructed by NCMBFs, is significantly optimized compared to CMBFM. Regrettably, the number of basis functions decreases from 4980 to 4797 after PCA handling.

In addition, both methods introduce the iLU decomposition technique to process the reduced matrix; this accelerates the iterative solution of the reduced matrix equation and diminishes the time
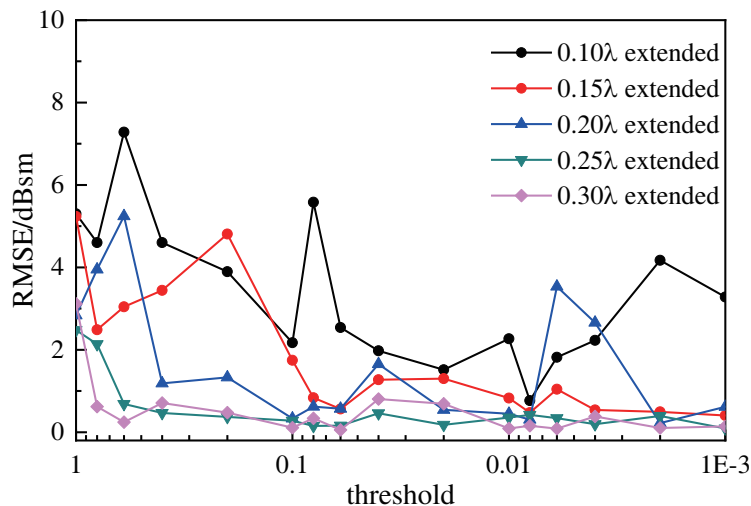
Figure 1. RMSE of CMBFM-PCA with different extended sizes.
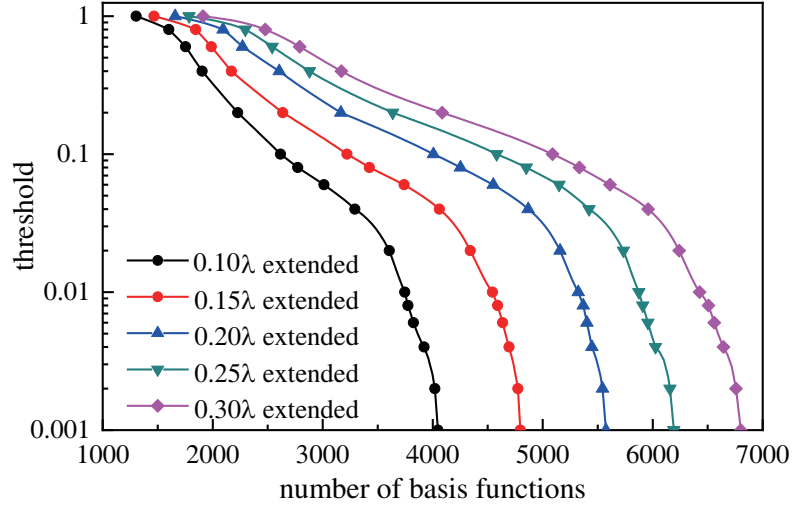
Figure 2. Variation of the number of NCMBFs with τ_{cm} in different extension sizes.
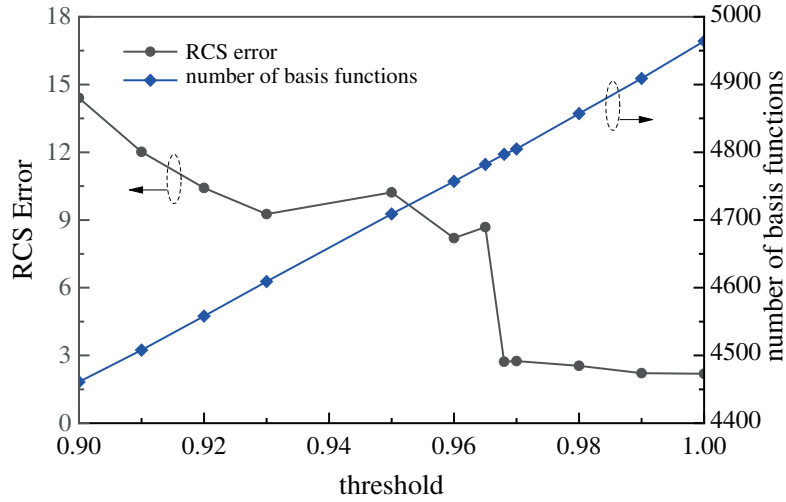
Figure 3. Variation of error and number of basis functions at different thresholds.

Table 1. Difference in condition number between CMBFM and CMBFM-PCA at different extension sizes.

Extended Size	Condition number of reduced matrix	
	CMBFM	CMBFM-PCA
0.10λ	2.7687E+06	1.3184E+04
0.15λ	1.0141E+08	2.0721E+04
0.20λ	6.6654E+08	3.4218E+04
0.25λ	3.9172E+09	2.4792E+04
0.30λ	1.2162E+10	1.2458E+05

cost. Consequently, the iteration numbers for solving the reduced matrix equation with the same threshold, using the two methods, are compared and presented in Fig. 4. Due to some advantages regarding the condition number of the reduced matrix in CMBFM-PCA, the iterative solution has fewer iterations; therefore, it converges faster. Furthermore, the calculation results of CBFM are added,
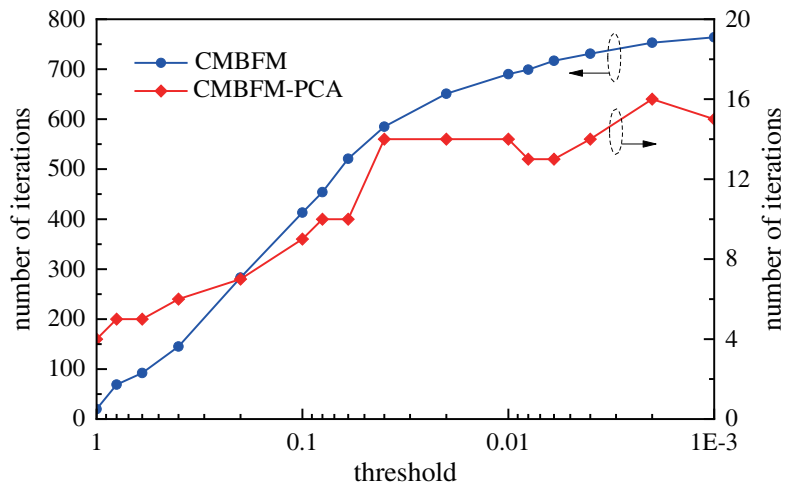
Figure 4. Number of iterations of the two methods with different thresholds.
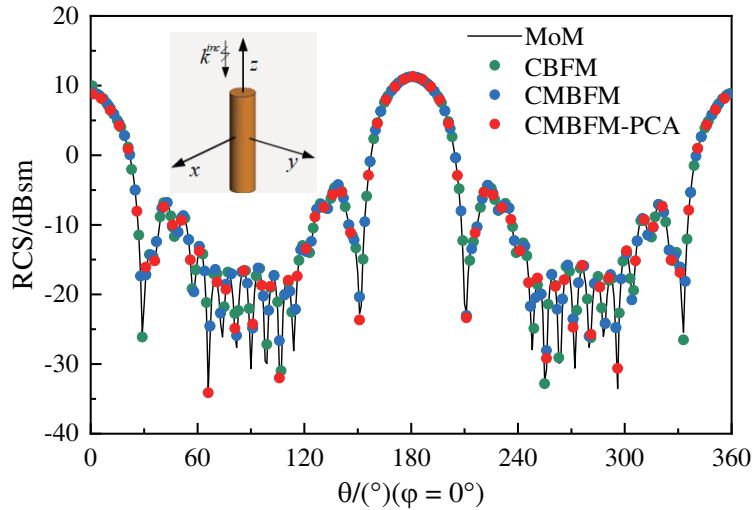
Figure 5. Bistatic RCS of cylinder in vertical polarization.

and the vertical polarized bistatic RCS of the cylinder is illustrated in Fig. 5. The results show that the calculated results of CMBFM-PCA have an excellent agreement with the MoM.

3.2. PEC Missile

Additionally, the bistatic RCS is calculated for a missile with a length of 1 m at a frequency of 3.5 GHz. The surface of the missile is discretized by the RWG function to produce 28864 triangles and 43296 unknowns. Afterwards, the target is divided into 55 blocks, and each one is extended by 0.15λ to obtain 91588 unknowns. Concerning the CMBFM-PCA, the thresholds for MS and PCA are set to 0.001 and 0.968, respectively, and the number of basis functions is decreased from 8548 to 8196. Simultaneously, the condition number of the reduced matrix decreases from 6.5771E+08 to 3.4137E+04 compared to CMBFM. Besides, the number of iterations needed to solve the reduced matrix equation is diminished from 875 to 44. In more detail, the horizontally polarized bistatic RCS of the missile is plotted in Fig. 6, and the results demonstrate that CMBFM-PCA has excellent computational accuracy.
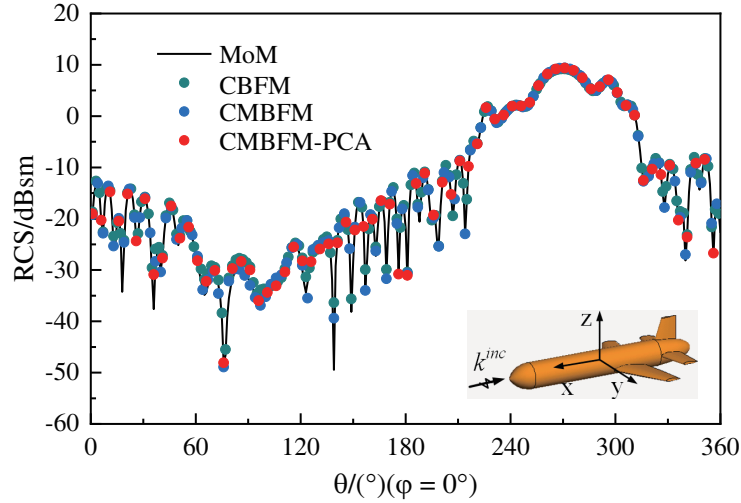
Figure 6. Bistatic RCS of missile in horizontal polarization.

3.3. PEC Cone-Sphere with a Gap

Finally, the bistatic RCS with a cone-sphere with a gap at an incident frequency of 6.7 GHz is calculated. The surface of the object is discretized by the RWG basis functions to create 32363 triangles and 48543 unknowns. Subsequently, the target is divided into 70 blocks, and each block is expanded by 0.15λ. The unknowns are increased to 101435. Likewise, the thresholds for MS and PCA are set to 0.001 and 0.968, respectively. Thus, the number of basis functions is reduced from 9733 to 9314, and the condition number is decreased from 6.6634E+07 to 7.4548E+03. Meanwhile, the iteration number for solving the matrix equation is diminished from 759 to 40. Furthermore, the vertical polarized bistatic RCS of the cone-sphere with a gap is shown in Fig. 7. It can be concluded that the proposed method is in a good agreement with the results of the MoM.
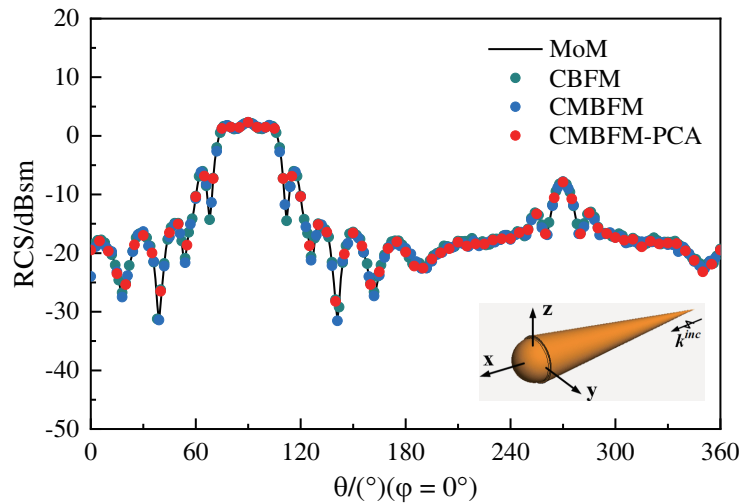
Figure 7. Bistatic RCS of cone-sphere with a gap in vertical polarization.

The simulation time of different processes and the corresponding RCS errors for Figs. 5, 6, and 7 are given in Table 2. Since the condition number of the reduced matrix is optimized, the time for an iterative solution is drastically reduced. Moreover, the total time of the three simulation experiments drops 36%, 44%, and 28%, respectively, and the computational efficiency is substantially improved while ensuring accuracy.

Table 2. The simulation time of different processes and RCS error.

Model	Method	Basis functions construction time (s)	Reduced matrix filling time (s)	Solving time (s)	Total time (s)	RCS Err (%)
Cylinder	CBFM	1842.9	483.5	57.4	3482.1	2.1
	CMBFM	163.7	211.3	676.1	2329.3	4.8
	Proposed method	167.0	199.4	22.9	1495.1	2.7
Missile	CBFM	2885.1	1134.6	127.7	7529.9	2.6
	CMBFM	304.8	872.9	1977.0	6033.2	3.4
	Proposed method	309.4	823.8	81.4	3420.0	4.5
cone-sphere with a gap	CBFM	4426.5	1958.2	178.6	14025.1	1.7
	CMBFM	655.7	1245.7	1793.2	9012.6	3.1
	Proposed method	666.9	1176.6	85.5	6546.7	2.2

4. CONCLUSION

In this paper, to solve the problems of slow convergence and low computational efficiency of the iterative solution of CMBFM in analyzing electrically large problems, CMBFM-PCA is proposed. The instruction of PCA, not only decreases the number of basis functions, but also enhances the orthogonality among them. Furthermore, the condition number of the reduced matrix is improved, and the convergence rate of the iterative solution is accelerated. Finally, numerical simulation results show the effectiveness of CMBFM-PCA, which effectively alleviates the difficulties of CM in analyzing electrically large targets.

ACKNOWLEDGMENT

REFERENCES

1. Harrington, R. F., *Field Computation by Moment Methods*, Macmillan, New York, 1968.
2. Bleszynski, E., M. Bleszynski, and T. Jaroszewicz, "Adaptive integral method for solving large-scale electromagnetic scattering and radiation problems," *Radio Sci.*, Vol. 31, No. 5, 1225–1251, Oct. 1996.
3. Zhao, K., M. Vouvakis, and J. F. Lee, "The adaptive cross approximation algorithm for accelerated MoM computations of EMC problems," *IEEE Trans. Electromagn. Compat.*, Vol. 47, No. 4, 763–773, Nov. 2005.
4. Tamayo, J. M., A. Heldring, and J. M. Rius, "Multilevel adaptive cross approximation (MLACA)," *IEEE Trans. Antennas Propag.*, Vol. 59, No. 12, 4600–4608, Dec. 2011.
5. Song, J. M. and W. C. Chew, "Multilevel fast multipole algorithm for solving combined field integral equations of electromagnetic scattering," *Microw. Opt. Technol. Lett.*, Vol. 10, No. 1, 14–19, Sep. 1995.

6. Lucente, E., A. Monorchio, and R. Mittra, "An iteration free MoM approach based on excitation independent characteristic basis functions for solving large multiscale electromagnetic scattering problems," *IEEE Trans. Antennas Propag.*, Vol. 56, No. 4, 999–1007, Apr. 2008.

7. Harrington, R. and J. Mautz, "Theory of characteristic modes for conducting bodies," *IEEE Trans. Antennas Propag.*, Vol. 19, No. 5, 622–628, Sep. 1971.

8. Gao, X., G. Tian, Z. Shou, and S. Li, "A low-profile broadband circularly polarized patch antenna based on characteristic mode analysis," *IEEE Antennas Wirel. Propag. Lett.* Vol. 20, No. 2, 214–218, Feb. 2021.

9. Fu, C., C. Feng, W. Chu, Y. Yue, X. Zhu, and W. Gu, "Design of a broadband high-gain omnidirectional antenna with low cross polarization based on characteristic mode theory," *IEEE Antennas Wirel. Propag. Lett.,* Vol. 21, No. 9, 1747–1751, Sep. 2022.

10. Lin, F. H. and Z. N. Chen, "Low-profile wideband metasurface antennas using characteristic mode analysis," *IEEE Trans. Antennas Propag.*, Vol. 65, No. 4, 1706–1713, Apr. 2017.

11. Angiulli, G., G. Amendola, and G. Di Massa, "Application of characteristic modes to the analysis of scattering from microstrip antennas," *Journal of Electromagnetic Waves and Applications*, Vol. 14, No. 8, 1063–1081, Jan. 2000.

12. Wang, P., Z. G. Wang, Y. F. Sun, et al., "A characteristic mode basis function method for solving wide angle electromagnetic scattering problems," *Journal of Electromagnetic Waves and Applications*, Vol. 36, No. 14, 1968–1979, Mar. 2022.

13. Jia, C., P. Gu, Z. He, et al., "Convergence acceleration of characteristic mode-based basis function method for connected array structures," *IEEE Trans. Antennas Propag.*, Vol. 70, No. 8, 7322–7327, Aug. 2022.

14. Wu, C., L. Guan, P. Gu, et al., "Application of parallel CM-MLFMA method to the analysis of array structures," *IEEE Trans. Antennas Propag.*, Vol. 69, No. 9, 6116–6121, Sep. 2021.

15. Jia, C., Z. He, M. Li, et al., "Characteristic mode-based efficient broadband electromagnetic scattering analysis method for array structures," *IEEE Geosci. Remote Sens. Lett.*, Vol. 19, 1–5, Oct. 2022.

16. Wang, Z. G., P. Wang, Y. F. Sun, et al., "Fast analysis of bistatic scattering problems for three-dimensional objects using compressive sensing and characteristic modes," *IEEE Antennas Wirel. Propag. Lett.*, Vol. 21, No. 9, 1817–1821, Sep. 2022..

17. He, R., B. G. Hu, W. S. Zheng, et al., "Robust principal component analysis based on maximum correntropy criterion," *IEEE Trans. Image Process.*, Vol. 20, No. 6, 1485–1494, Jun. 2011.

18. Gu, T., "Detection of small floating targets on the sea surface based on multi-features and principal component analysis," *IEEE Geosci. Remote Sens. Lett.*, Vol. 17, No. 5, 809–813, May 2020.

19. Hao, T., L. Jing, and W. He, "An automated GPR signal denoising scheme based on mode decomposition and principal component analysis," *IEEE Geosci. Remote Sens. Lett.*, Vol. 20, 1–5, Dec. 2022.